



Preparation and Characterization of Polyethylene Glycol Coating Iron Oxide Nanoparticles for Curcumin Delivery

NGUYEN THI THANH THUY^{1,*}, LE DUC ANH¹, NGUYEN HUU TRI², CU VAN HOANG¹ and NGUYEN ANH NHUT¹

¹Department of Chemistry, Nong Lam University, Ho Chi Minh City, Vietnam

²Department of Natural Resources and Environment, Dong Nai Province, Vietnam

*Corresponding author: Tel: +84 918 945711; E-mail: nguyenthanhthuy@hcmuaf.edu.vn

Received: 18 January 2019;

Accepted: 16 March 2019;

Published online: 28 June 2019;

AJC-19441

The PEG-coated iron oxide nanoparticles (Fe₃O₄ NPs-PEG) was synthesized by coprecipitation and ultrasonication method. X-ray diffraction results exhibited that the average size of Fe₃O₄ NPs-PEG was 19.10 nm, which was further confirmed in TEM imaging. In addition, sonication time and curcumin concentration were studied to evaluate the efficiency of loading curcumin onto Fe₃O₄ NPs-PEG. Further, statistical optimization using response surface methodology (RSM) has shown curcumin concentration (0.01% w/v) and sonication time (21 min) for maximal curcumin loading (0.37 mg/g). Along with the magnetization studies, the immobilization of curcumin onto the Fe₃O₄ NPs-PEG was characterized by UV, FTIR and SEM. The results showed that the curcumin loaded PEG coated iron oxide nanoparticles could potentially be used for magnetically target drug delivery.

Keywords: Curcumin, Iron oxide nanoparticles, Polyethylene glycol, Response surface methodology, Sonication.

INTRODUCTION

In recent year, iron oxide nanoparticles are increasingly used in many fields due to their remarkable properties such as super paramagnetism, size, surface and biocompatible [1]. These special characteristics make them an attractive platform for a variety of biomedical and bioengineering application including cell separation and detection [2], cancer treatment [3], hyperthermia [4], drug delivery [5] and contrast agents in magnetic resonance imaging (MRI) [6]. Owing to the unique properties and great potential of iron oxide nanoparticles for bio-application, it would be interesting to study their magnetic properties. However, iron oxide nanoparticles have many disadvantages, as they have tendency to appear aggregation due to van der Waals and strong dipole-dipole interactions [7]. Therefore, it is important to combine iron oxide nanoparticles with a suitable coating such as dextran, polyvinyl alcohol (PVA), chitosan, polyethylene glycol (PEG), polyvinylpyrrolidone (PVP), polylactic-co-glycolic acid (PLGA), etc. to improve their stabilization [8-12].

In this study, curcumin (Cur) was used to load onto surface iron oxide nanoparticles stabilized polyethylene glycol

(Cur-Fe₃O₄ NPs-PEG) as a potential drug delivery for magnetically medicated targeted anticancer therapy. Polyethylene glycol is known to be a water-soluble, hydrophilic, non-antigenic, and biocompatible polymer [13]. Curcumin is a kind of polyphenol derivatives, which is natural product extracted from turmeric (*Curcuma longa*). It is proved that curcumin has general biological and pharmaceutical activity, which is a green and non-toxic in nature [14].

In this investigation, Cur-Fe₃O₄ NPs-PEG were subjected to a series of characterization studies to determine their size, structure and morphology using by X-ray diffraction, Fourier transform infrared spectroscopy, UV-vis, scanning electron microscopy and transmission electron microscopy.

EXPERIMENTAL

Iron(II) chloride tetrahydrate (FeCl₂·4H₂O) (≥ 99 %, Merck KgaA-German), iron(III) chloride hexahydrate (FeCl₃·6H₂O) (≥ 99 %, Merck KgaA-German), ammonia solution (25 % wt. %), sodium citrate (Xilong, China), NaOH (Merck), polyethylene glycol (PEG, number average molecular weight, M_n = 2000 g/mol, PEG2000, Merck KgaA, German), curcumin (97 %),

acetone and dimethyl sulfoxide (Xilong Scientific Co., Ltd, China) were used as such. Deionized water was used throughout the experiment.

Synthesis of PEG coated iron oxide nanoparticles (Fe₃O₄ NPs-PEG): PEG coated iron oxide nanoparticles were synthesized by co-precipitation and ultra-sonication methods. A mixed solution of ferric and ferrous ions was prepared by dissolving 2.705 g FeCl₃·6H₂O and 0.995 g FeCl₂·4H₂O in 50 mL of distilled water. Then, 3 g of C₆H₅Na₃O₇ and 10 mL NH₃ solution (25%) was added dropwise until pH = 9 to above solution at 80 °C and sonicated for 2 h. After, 10 g PEG was dissolved into 50 mL distilled water and added drop by drop to solution using a magnetic stirrer for 24 h at ambient temperature. Coated particles were separated using a permanent magnet and washed with distilled water. This procedure was repeated several times in order to remove excess polymer. Obtained PEG coated iron oxide nanoparticles was a black power after drying at room temperature for 1 day and store before being characterized.

Immobilization of curcumin onto Fe₃O₄ NPs-PEG: Loading curcumin onto the surface Fe₃O₄ NPs-PEG was carried out by dispersing 50 mg of PEG coated iron oxide nanoparticles in 10 mL of curcumin solution following the experimental procedure described by Cheng *et al.* [15]. The mixture of PEG coating iron oxide nanoparticles in curcumin solution was sonicated and combined with vortex for 20 min. Then, the solution was adjusted to pH = 5.5 using ascorbic acid. The solution was stirred continuously for 24 h at ambient temperature to enhance the penetration of curcumin onto Fe₃O₄ NPs-PEG. The curcumin loading Fe₃O₄ NPs-PEG was centrifuged for 30 min and the amount of free curcumin in clear supernatant was analyzed by UV-visible spectrophotometer at the wavelength of 420 nm. Obtained nanoparticles were washed three times with acetone and distilled water with the help of magnets. The curcumin loading was determined according to the following eqn. 1:

$$q = \frac{(C_0 - C)V}{m} \quad (1)$$

where q is the amount of curcumin loading onto nanoparticles (mg/g), C₀ is the initial concentration of curcumin (mg/L), C is the concentration of curcumin in supernatant (mg/L), V is the volume of solution (L), and m is the mass of nanoparticles (g).

Experimental design: To optimized the conditions of preparation of curcumin loading onto surface Fe₃O₄ NPs-PEG,

response surface methodology (RSM) and central composite rotatable design (CCRD) were used to estimate the main effects on response, *i.e.* the efficiency of percent loading curcumin to Fe₃O₄ NPs-PEG. Loading curcumin onto nanoparticles was executed under three different curcumin concentrations: C1 (0.005 %), C2 (0.010 %), C3 (0.015 %). Time of sonication was varied as t₁ (10 min), t₂ (20 min), t₃ (30 min). Two factors with three levels consisting of nine experimental runs were used to analyze the experimental data including three replicates at the center point [16]. Curcumin concentration (C %) and time of sonication (t) were chosen as the experimental factors or the independent variables capable of influencing the percentage of curcumin loading (Y). Analysis was done using coded values as -1, 0 and +1. Using this design, the experimental data were fitted according to equation (2) as a second-order polynomial equation including individual and cross-effects of variable.

$$Y = a_0 + a_1X_1 + a_2X_1^2 + a_3X_2 + a_4X_2^2 + a_5X_1X_2 \quad (2)$$

where a₀, a₁, a₂, a₃, a₄, a₅ are regression coefficients, Y is the curcumin loading contents (response), X₁ is concentration of curcumin, X₂ is time of sonication. The data (Table-1) were the averages of the measurements. Multiple regression analysis, response surface plots and statistical analyses were performed using JMP 10 software.

Characterizations: The size and morphological characterization of the nanoparticles were carried out using a JEOL 2010 transmission electron microscope (TEM) operating at 200 kV. UV spectra were analyzed by a Genesys 20 (Thermo Scientific Genesys: USA). The FTIR spectra were measured in a Nicolet (Impact 410, Madison, WI), FTIR spectrophotometer by KBr pellets. The crystallite phase of the particles was identified by recording X-ray diffraction patterns (XRD) using a Shimadzu XRD-6000 X-ray diffractometer with Cu-Kα radiation source. The hydrodynamic diameter of nanoparticles was determined by dynamic light scattering at a fixed scattering angle of 90° with a Zetasizer Nano (Malvern, UK) at 25 °C.

RESULTS AND DISCUSSION

The X-ray diffractogram data matched the pattern of bulk magnetic (Fig. 1a). A characteristic peak was obtained for Fe₃O₄ at a 2θ value of 30.39°, 35.66°, 43.34°, 53.80°, 57.34°, 63.01° corresponding to (220), (311), (400), (511), and (440) [17]. No peak was observed for any impurities. The same pattern was observed with Fe₃O₄ NPs-PEG (Fig. 1b). This indicated that the

TABLE-1
VARIABLE PARAMETERS FOR THE STATISTICAL ANALYSIS, OBSERVED AND PREDICTED VALUES OR RESPONSE (CURCUMIN LOADING CONTENTS)

Run	Real values		Coded values		Observed response	Predicted response
	Curcumin concentration (%) (X ₁)	Time of sonication (min) (X ₂)	Curcumin concentration (%) (U ₁)	Time of sonication (min) (U ₂)		
1	0.005	10	-1	-1	0.127000	0.133908
2	0.005	20	-1	0	0.186000	0.171407
3	0.005	30	-1	+1	0.137667	0.145352
4	0.010	10	0	-1	0.346667	0.340852
5	0.010	20	0	0	0.366000	0.379185
6	0.010	30	0	+1	0.361333	0.353963
7	0.015	10	+1	-1	0.176667	0.175574
8	0.015	20	+1	0	0.213333	0.214741
9	0.015	30	+1	+1	0.190667	0.190352

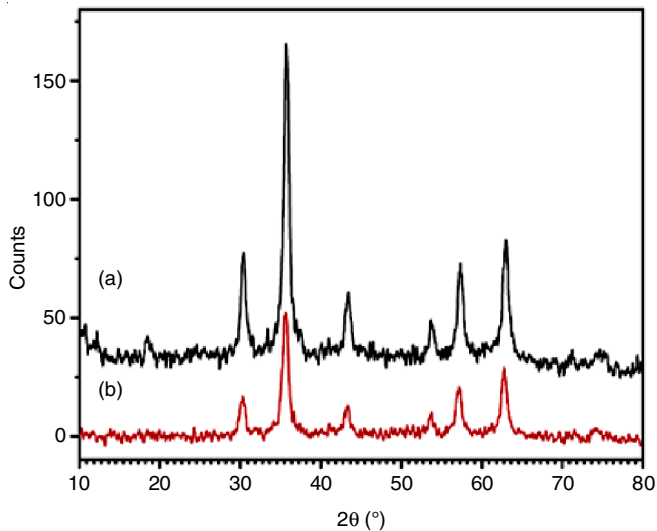


Fig. 1. X-ray powder diffraction pattern of (a) Fe_3O_4 NPs and (b) Fe_3O_4 NPs-PEG

coating PEG did not affect crystalline structure of magnetite. Furthermore, the peak intensity of Fe_3O_4 NPs-PEG was lower than that of bare iron oxide nanoparticles, which revealed to the existence of PEG coated on surface of iron oxide nanoparticles. The mean crystallite size has been calculated by Scherrer's formula [18] (eqn. 3):

$$D = \frac{0.9\lambda}{\beta \cos \theta} \quad (3)$$

where D is the crystalline domain size, K is the Scherrer constant ($K = 0.9$ in this case), λ is the wavelength of X-ray ($\lambda = 1.574 \times 10^{-10} \text{ m} = 1.54060 \text{ \AA} = 0.154060 \text{ nm}$), β is the peak angular width and θ is the diffraction angle.

The mean crystallite size of iron oxide nanoparticles with and without coated PEG was 11.8268 nm and 17.0230 nm, respectively. The TEM images of bare iron nanoparticles and the PEG coated onto magnetite surface are shown in Fig. 3, confirmed the formation of crystalline nanoparticles. The diameter of the bare magnetite and Fe_3O_4 NPs-PEG was calculated manually from the TEM images and determined to be 12.155 and 19.107 nm, respectively which was in good agreement with the XRD results. FTIR analysis was performed to determine the presence of PEG layer on nanoparticles surface. Fig. 2 shows the FTIR spectrum of bare iron oxide nanoparticles, PEG coated iron oxide nanoparticles and PEG 2000. In case of bare iron oxide nanoparticles, the band at 585 cm^{-1} is assigned to the stretching vibration of Fe-O in Fe_3O_4 [19] and the peak at broad vibration band between 3415 and 3500 cm^{-1} corresponded to the OH stretching vibrations of water molecules which is assigned to -OH adsorbed by particles [20].

In the FTIR spectrum of PEG, peak at 2887 cm^{-1} corresponded to the stretching vibration of $-\text{CH}_2$, the peak at 1114 cm^{-1} is assigned to the vibration of C-O, at 963 cm^{-1} the C-C stretch band was observed, the peak at 3429 cm^{-1} attributed to the stretching vibration of OH band. The FTIR of PEG coated nanoparticles was identical with that of PEG pure, except the band at 585 cm^{-1} has appeared which corresponded to the stretching vibration of Fe-O bond. All these finding complete confirmed the presence of PEG onto nanoparticles surface.

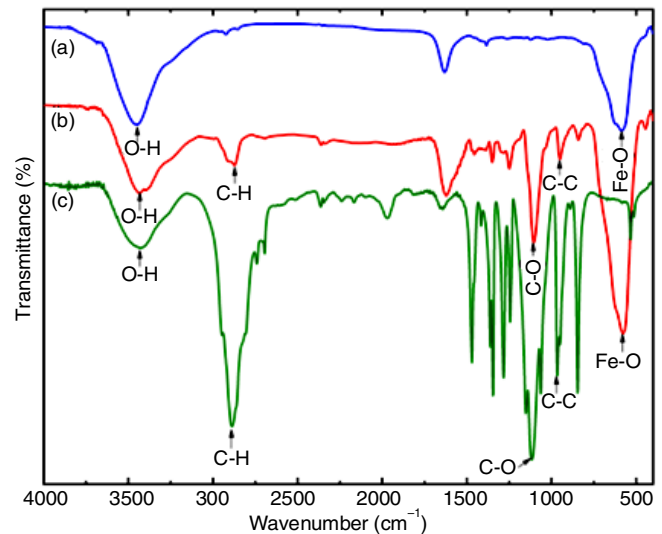


Fig. 2. FTIR spectrum of (a) Fe_3O_4 NPs, (b) Fe_3O_4 NPs-PEG and (c) PEG-2000

DLS measurement showed that the average diameters of bare Fe_3O_4 and Fe_3O_4 NPs-PEG were 66.3 ± 22.1 and 86.9 ± 31.2 , respectively (Fig. 3). Particle size measured by DLS was larger than that measured by TEM. The difference between DLS and TEM data was explained by the fact that DLS experiment was carried out in solution whereas TEM images were taken in a dried state (Fig. 3). The central composite rotatable design (CCRD) was used to determine the correlation of experimental variables and the loading curcumin contents.

The empirical relationships between the curcumin loading contents and the two variables in coded units obtained by eqn 4:

$$Y = 0.379185 + 0.021667X_1 - 0.186111X_1^2 - 0.031777X_2^2 \quad (4)$$

All two variables chosen (curcumin concentration and time of sonication) had a quadratic effect on the loading curcumin contents (Fig. 4). It was clearly shown that the predicted values were fitted well with the actual values. Tables 2 and 3 showed that the time of sonication and the curcumin concentration have influenced significantly to the loading curcumin onto nanoparticles surface.

TABLE-2
MODEL COEFFICIENT ESTIMATED
BY MULTIPLE REGRESSION

Factor	Coefficient	t-value	p-value
Constant	0.379185	36.43	0.0000 < 0.05
U_1	0.0216667	3.80	0.0320 < 0.05
U_2	0.0065555	1.15	0.3335 > 0.05
$U_1 * U_2$	0.0008332	0.12	0.9125 > 0.05
$U_1 * U_1$	-0.186111	-18.85	0.0003 < 0.05
$U_2 * U_2$	-0.031777	-3.22	0.0486 < 0.05

TABLE-3
OPTIMIZED RESULTS OF THE INFLUENCE OF
CURCUMIN CONCENTRATION AND TIME OF
SONICATION TO LOADING CURCUMIN CONTENTS

Factors	Proposed value	Rounding value
Curcumin concentration (0.005/0.015)	0.0102922	0.01
Time of sonication (10.30)	21.039131	21
Loading curcumin contents predicted	0.3801587	
Loading curcumin contents obtained	0.371±0.007	

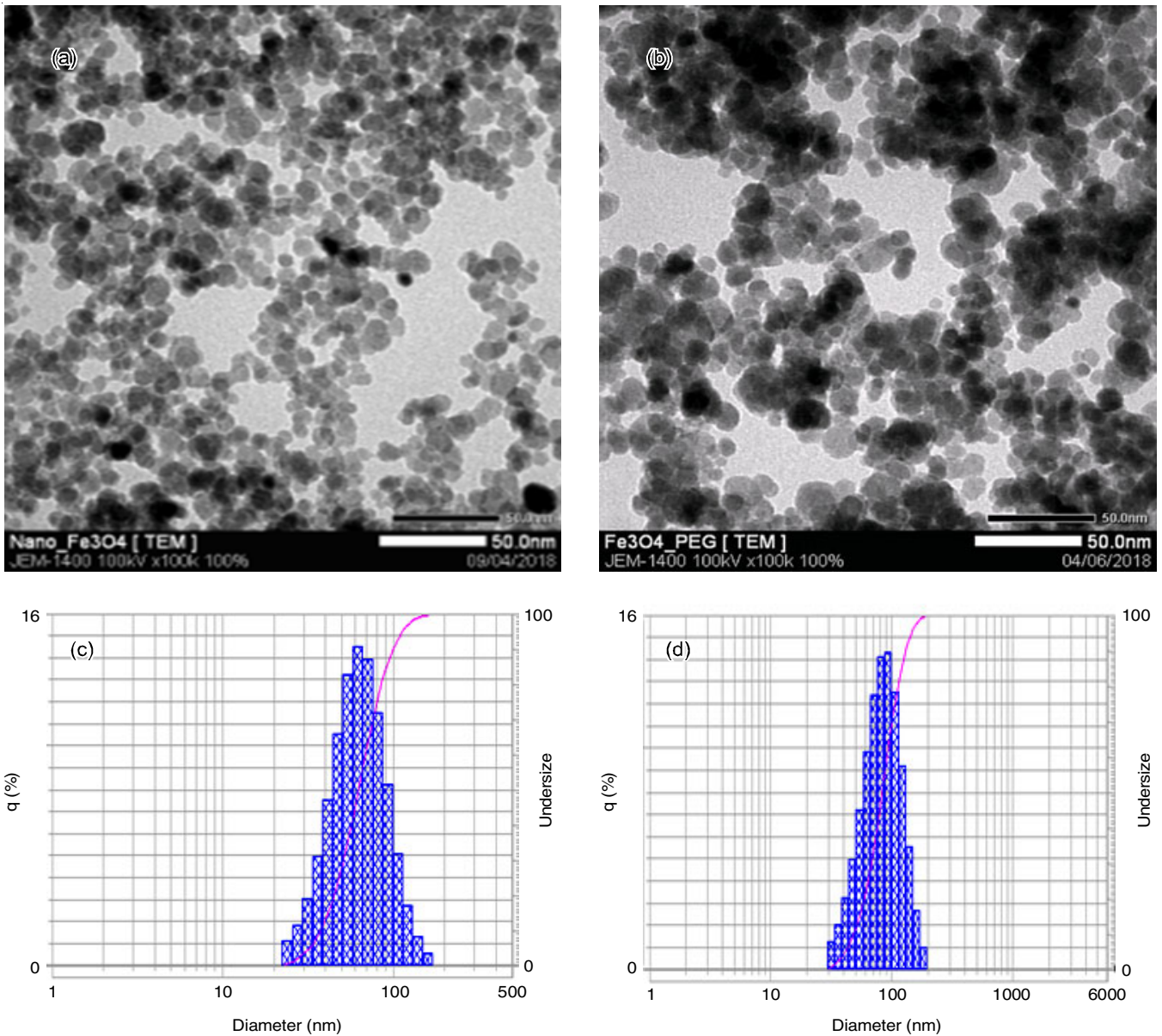


Fig. 3. TEM micrographs of (a) Fe₃O₄ NPs, (b) Fe₃O₄ NPs-PEG with their size distribution determined by DLS

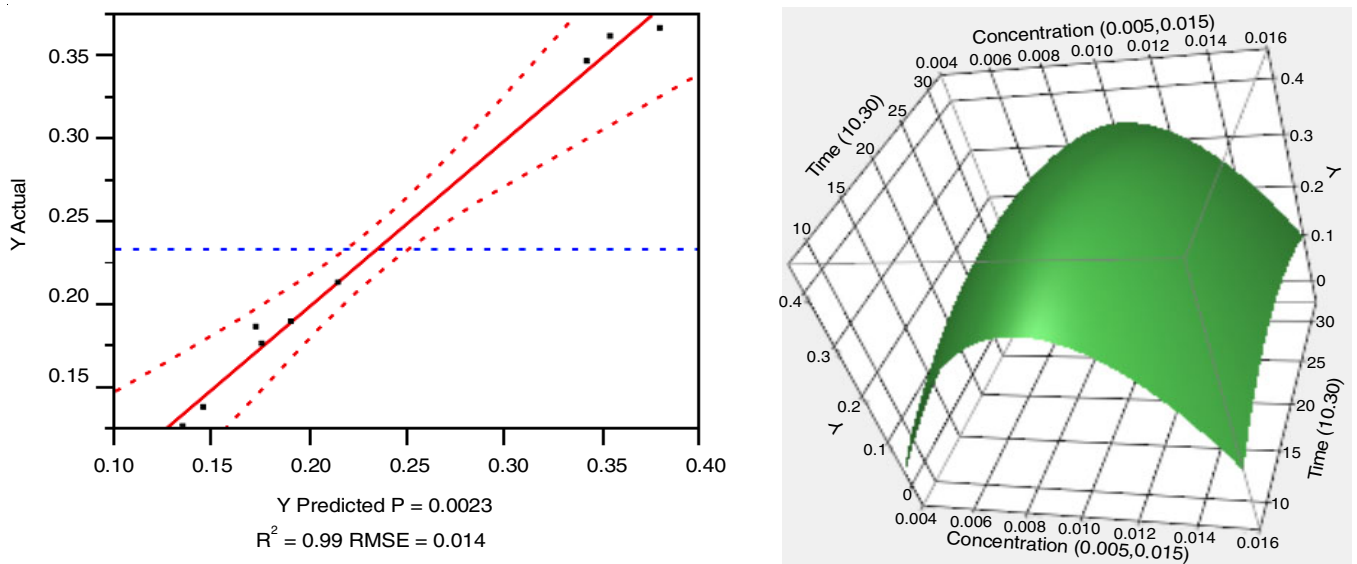


Fig. 4. Actual result *versus* predicted result

FTIR was further extended to study the loading of curcumin with PEG coated iron oxide nanoparticles. FTIR spectra of curcumin alone and curcumin loaded PEG coated iron oxide nanoparticles are shown in Fig. 5. FTIR spectrum of curcumin shows broad peak round at $3500\text{--}3390\text{ cm}^{-1}$ due to the -OH stretching vibration. The peaks at 1627 , 1602 and 1509 cm^{-1} were attributed to the C=O, C=C, C-O-C stretching vibrations, respectively. The Cur- Fe_3O_4 NPs-PEG inherited the characteristic peaks of PEG, Cur and Fe_3O_4 as C-H at 2.885 cm^{-1} and C-O-C at 1.114 cm^{-1} for PEG, C=O at 1.627 cm^{-1} for Cur and Fe-O at 578 cm^{-1} for Fe_3O_4 . These results showed that there is existence an interaction between curcumin, PEG and magnetite.

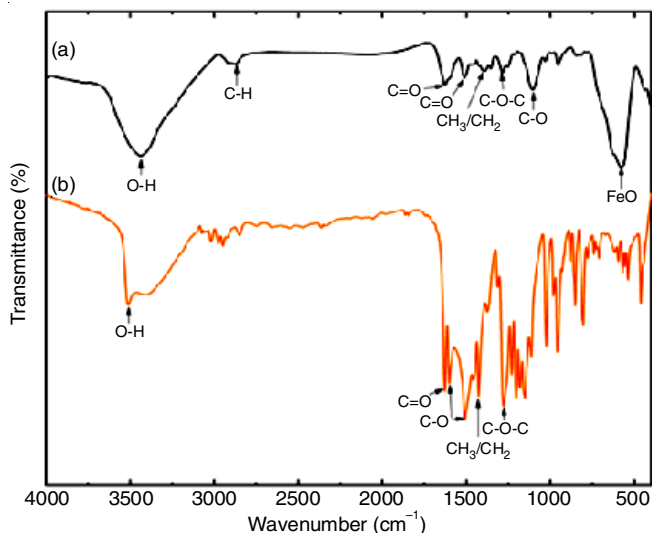


Fig. 5. FTIR spectra of (a) pure curcumin and (b) curcumin loaded Fe_3O_4 NPs-PEG

The surface morphology of Cur-loaded Fe_3O_4 NPs-PEG is shown in Fig. 6. It is seen that the particles were uniformly distributed. The curcumin loaded Fe_3O_4 NPs-PEG showed a rough spherical structure. The SEM morphology also showed that curcumin embedded onto PEG coated iron oxide nanoparticles.

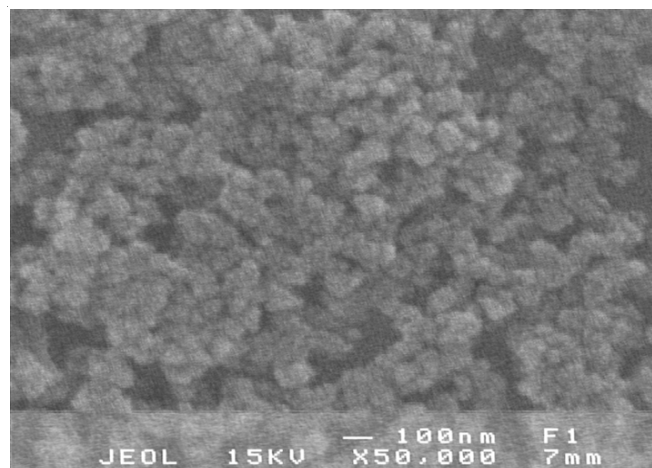


Fig. 6. SEM image of curcumin-loaded Fe_3O_4 NPs-PEG

Conclusion

In the present study, curcumin loaded onto biocompatible polyethylene glycol coating iron oxide nanoparticles was synthe-

sized by co-precipitation-ultrasonication methods. Nanoparticles were characterized by FTIR, TEM, SEM and XRD. The results were adapted each other. According to X-ray diffraction studies, it was found that the size of Fe_3O_4 NPs-PEG was larger than that of bare nanoparticles due to PEG coated on magnetite surface. The curcumin loaded PEG coated iron oxide nanoparticles are promising for biomedical applications such as magnetic drug carriers.

ACKNOWLEDGEMENTS

This work was supported by Nong Lam University, Ho Chi Minh City, Vietnam under research project code CS-CB17-KH-02.

CONFLICT OF INTEREST

The authors declare that there is no conflict of interests regarding the publication of this article.

REFERENCES

- A.H. Lu, E.L. Salabas and F. Schüth, *Angew. Chem. Int. Ed.*, **46**, 1222 (2007); <https://doi.org/10.1002/anie.200602866>.
- C. Yang, A. Rait, K.F. Pirolo, J.A. Dagata, N. Farkas and E.H. Chang, *Nanomed.-Nanotechnol.*, **4**, 318 (2008); <https://doi.org/10.1016/j.nano.2008.05.004>.
- Y. Ling, K. Wei, Y. Luo, X. Gao and S. Zhong, *Biomaterials*, **32**, 7139 (2011); <https://doi.org/10.1016/j.biomaterials.2011.05.089>.
- Z.-Q. Zhang and S.-C. Song, *Biomaterials*, **106**, 13 (2016); <https://doi.org/10.1016/j.biomaterials.2016.08.015>.
- C. Saikia, M.K. Das, A. Ramteke and T.K. Maji, *Int. J. Biol. Macromol.*, **93**, 1121 (2016); <https://doi.org/10.1016/j.ijbiomac.2016.09.043>.
- A. Mashhadi Malekzadeh, A. Ramazani, S.J. Tabatabaei Rezaei and H. Niknejad, *J. Colloid Interface Sci.*, **490**, 64 (2017); <https://doi.org/10.1016/j.jcis.2016.11.014>.
- S. Theerdhala, D. Bahadur, S. Vitta, N. Perkas, Z. Zhong and A. Gedanken, *Ultrason. Sonochem.*, **17**, 730 (2010); <https://doi.org/10.1016/j.ultsonch.2009.12.007>.
- L. Ngaboni Okassa, H. Marchais, L. Douziech-Eyrolles, S. Cohen-Jonathan, M. Soucé, P. Dubois and I. Chourpa, *Int. J. Pharm.*, **302**, 187 (2005); <https://doi.org/10.1016/j.ijpharm.2005.06.024>.
- B.R. Jarrett, M. Frendo, J. Vogan and A.Y. Louie, *Nanotechnology*, **18**, 035603 (2007); <https://doi.org/10.1088/0957-4484/18/3/035603>.
- L. Li, D. Chen, Y. Zhang, Z. Deng, X. Ren, X. Meng, F. Tang, J. Ren and L. Zhang, *Nanotechnology*, **18**, 405102 (2007); <https://doi.org/10.1088/0957-4484/18/40/405102>.
- M. Mahmoudi, A. Simchi, M. Imani, A.S. Milani and P. Stroeve, *J. Phys. Chem. B*, **112**, 14470 (2008); <https://doi.org/10.1021/jp803016n>.
- A. Masoudi, H.R. Madaah Hosseini, M.A. Shokrgozar, R. Ahmadi and M.A. Oghabian, *Int. J. Pharm.*, **433**, 129 (2012); <https://doi.org/10.1016/j.ijpharm.2012.04.080>.
- M. Mahmoudi, A. Simchi, A. Milani and P. Stroeve, *J. Colloid Interface Sci.*, **336**, 510 (2009); <https://doi.org/10.1016/j.jcis.2009.04.046>.
- C. Araujo and L. Leon, *Mem. Inst. Oswaldo Cruz*, **96**, 723 (2001); <https://doi.org/10.1590/S0074-02762001000500026>.
- K.K. Cheng, P.S. Chan, S. Fan, S.M. Kwan, K.L. Yeung, Y.-X.J. Wang, A.H.L. Chow, E.X. Wu and L. Baum, *Biomaterials*, **44**, 155 (2015); <https://doi.org/10.1016/j.biomaterials.2014.12.005>.
- R. Konwarh, J.P. Saikia, N. Karak and B.K. Konwar, *Colloid Surf. B*, **81**, 578 (2010); <https://doi.org/10.1016/j.colsurfb.2010.07.062>.
- S. García-Jimeno and J. Estelrich, *Colloid Surf. A*, **420**, 74 (2013); <https://doi.org/10.1016/j.colsurfa.2012.12.022>.
- B. Cullity and S. Stock, *Elements of X-Ray Diffraction*, Upper Saddle River, NJ: Prentice Hall, edn 3 (2001).
- R. Ahmadi, M. Malek, H.R.M. Hosseini, M.A. Shokrgozar, M.A. Oghabian, A. Masoudi, N. Gu and Y. Zhang, *Mater. Chem. Phys.*, **131**, 170 (2011); <https://doi.org/10.1016/j.matchemphys.2011.04.083>.
- A.K. Gupta and S. Wells, *IEEE T. Nanobiosci.*, **3**, 66 (2004); <https://doi.org/10.1109/TNB.2003.820277>.